

IMECE2003-41421

MULTIDIMENSIONAL HIDDEN SLOW VARIABLE TRACKING IN A HIERARCHICAL DYNAMICAL SYSTEM

David Chelidze

Department of Mechanical Engineering and Applied Mechanics
University of Rhode Island
Kingston, Rhode Island 02881
Email: chelidze@egr.uri.edu

ABSTRACT

In this paper, we present a novel method for multidimensional damage identification based on a dynamical systems approach to damage evolution. This approach does not depend on the knowledge of particular damage physics, and is appropriate for systems where damage evolves on much slower time scale than the directly observable dynamics. In an experimental context, the phase space reconstruction and locally linear models are used to quantify small distortions occurring in a dynamical system's phase space due to damage accumulation. These measurements are then related to the drifts in damage variables. A mathematical model of a harmonically driven cantilever beam in a force field of two battery-powered electromagnets is used to demonstrate validity of the method. It is explicitly demonstrated that an affine projection of the described damage metric accurately tracks the two competing damage processes. For practical damage identification purposes, the tracking data is analyzed using the proper orthogonal decomposition (POD) and optimal tracking (OT) methods. Both methods correctly identify the two dominant damage modes. However, the OT is more impervious to changes in fast-time dynamics and provides a significantly better signal-to-noise ratio. The OT-based damage observer is demonstrated to be within a linear transformation from the actual damage states.

INTRODUCTION

The development of machinery and structural health monitoring technology is one of the important tasks of current applied engineering research. This is a formidable undertaking, consid-

ering the complex and hidden nature of damage. Damage can refer to any variety of physical processes that cause degradation in a system's performance leading to imminent failures. Existing literature abounds with solutions to some particular *imminent damage* detection problems (e.g., material fracture, sensor or power source failure, etc.) that mainly focus on scalar damage processes. Current research efforts, however, move past such alarm-based diagnostics of scalar variables to *gray scale* health monitoring of *incipient* multi-valued damage processes, which is required for the development of true prognostic ability.

Most of the early mechanical systems damage identification work focused on damage detection [1]. Data-based, or heuristic, approach is to look for changes due to the damage accumulation in time or frequency domain statistics [2], or in statistics that have both time and frequency information [3]. For nonlinear systems exhibiting chaotic response it is customary to use estimates of long-time chaotic invariant measures, such as the correlation dimension [4]. Other advanced techniques use expert systems or fuzzy logic [5]. The main advantages of such methods are simplicity of implementation and that they often work very well. Most heuristic methods serve as purely damage detection methods; i.e., no damage state assessment is provided. Even when the severity of damage can be estimated [6], it is usually very hard to establish a direct one-to-one connection between the damage state and the change in the heuristic statistic or feature vector. There is no theoretical basis for predicting a priori, without the benefit of a good model or experiment, whether a certain feature vector will work well for a particular system.

A model-based approach addresses some of the shortcom-

ings of the purely statistical approach at the expense of a more difficult development and implementation [7]. In rare cases, when the system's analytical model is available, it is usually possible to establish a functional connection between the drifting model parameters and a particular feature vector [8]. The lack of analytical models is customarily addressed by developing finite elements or data-based models. For linear systems, for example, autoregressive model parameter spectra and linear prediction error are used for fault detection in ball bearings [9] and gears [10], respectively. As another example, the frequency response functions are widely used for damage detection [11] in structures. Nonlinear systems are usually modeled using neural networks [12] for the same purpose. Other successful approaches are based on some type of hybrid method. For example, extensive attention is allotted to the use of mode shapes, or their curvatures, for damage detection and identification [13]. However, in many cases these methods are application dependent, and the main advantage of a model-based approach, which is to correlate the changes in a feature vector with the changes in a system's physical parameters, is lost.

In this paper, a novel multidimensional damage diagnosis method is developed. It is based on a dynamical systems approach to damage evolution [14]. Damage diagnosis is accomplished using a novel concept of phase space warping [15–17], which refers to small distortions in the phase space of a system due to the damage accumulation. The method presented here is able to track competing damage modes that evolve on much slower time scales than the directly observable dynamics of a system. For systems undergoing abrupt changes the method is not able to provide tracking. However, it can still detect and quantify these changes.

In the next section, a brief description of the dynamical systems approach to damage evolution is given. A new multidimensional damage tracking metric is introduced next, and a novel strategy for damage identification is described. Application of the proposed techniques to a model of an electromechanical system with drifting potential field is described next. The results of two-dimensional damage identification and their implications are discussed at the end, followed by conclusions.

DYNAMICAL SYSTEMS APPROACH TO DAMAGE EVOLUTION

In the dynamical systems approach [14], damage is viewed as a point evolving in an extended phase space of a hierarchical dynamical system. In this system, slow-time damage evolution causes parameter drifts in a subsystem describing dynamics of directly observable fast-time variables:

$$\dot{\mathbf{x}} = \mathbf{f}(\mathbf{x}, \boldsymbol{\mu}(\phi)), \quad (1a)$$

$$\dot{\phi} = \epsilon \mathbf{g}(\phi, \mathbf{x}), \quad (1b)$$

where: $\mathbf{x} \in \mathbb{R}^n$ is a directly observable, fast-time variable; $\phi \in \mathbb{R}^m$ is a hidden damage, slow-time variable; $\boldsymbol{\mu} \in \mathbb{R}^s$ is a function of ϕ representing the parameters in Eq. (1a); a rate constant $0 < \epsilon \ll 1$ defines a time-scale separation between fast- and slow-time dynamics; and overdots denote differentiation with respect to time t . Note that, for $\epsilon = 0$ the parameter vector $\boldsymbol{\mu}$ is a constant and system Eq. (1a) is stationary, and for $\epsilon \neq 0$ Eq. (1a) is nonstationary due to the evolution of ϕ . However, over the time scales of $\mathcal{O}(\epsilon)$ we consider Eq. (1a) to be quasistationary, since drifts in $\boldsymbol{\mu}$ are negligible.

This formulation is appropriate for systems where damage accumulation can be characterized by a time scale that is several orders of magnitude larger than a time scale associated with dynamic response of a corresponding structure. In the following, we develop main ideas behind multidimensional damage tracking strategy.

The Phase Space Warping Tracking Function

In an experimental context we usually do not have access to the analytical form of governing differential equations (1). However, we do have access to measurements from the fast-time system (1a). These measurements are usually sampled at uniform time intervals t_s , and the dynamics (i.e., the equivalent topological structure of the extended phase space) of Eq. (1a) can be reconstructed using a delay coordinate embedding [18]. In this procedure, the measured scalar time series $\{x(r)\}_{r=1}^M$ is converted to a series of vectors $\mathbf{y}^T(r) = [x(r), x(r + \tau), \dots, x(r + (d - 1)\tau)] \in \mathbb{R}^d$, where τ (multiple of t_s) is a suitable delay time, and d is the appropriate embedding dimension. Embedding parameters, τ and d , are usually determined using the first minimum of the average mutual information [19] and method of false nearest neighbors [20], respectively.

The reconstructed state vectors are governed by an as yet unknown map of the form

$$\mathbf{y}(r + 1) = \mathbf{P}(\mathbf{y}(r); \phi). \quad (2)$$

The drift in the damage variable ϕ will cause distortions in the phase space, altering the evolution of trajectories. The *phase space warping* (PSW) refers to these changes in the vector field. In previous work [15, 16], the following *PSW tracking function*

$$\mathcal{E}_k(\mathbf{y}(r), \phi) = \mathbf{P}^k(\mathbf{y}(r), \phi) - \mathbf{P}^k(\mathbf{y}(r), \phi_0) \quad (3)$$

was proposed for damage identification. In Eq. (3) \mathbf{P}^k is the k -th iterate of the map defined by Eq. (2).

Note that, for fixed $\mathbf{y}(r)$, the PSW tracking function can be expanded into a Taylor series in ϕ . For ϕ sufficiently close to ϕ_0 , it is shown in [15] that, assuming *linear observability* (i.e., assuming the first derivative of \mathbf{P}^k with respect to ϕ has maximal

rank), the relationship between the PSW tracking function and the damage variable can be well-approximated by an affine map

$$\mathcal{E}_k(\mathbf{y}(r), \phi) = \mathbf{C}(\mathbf{y}(r))\phi + \mathbf{c}(\mathbf{y}(r)), \quad (4)$$

where the matrix $\mathbf{C} = \partial \mathbf{P}^k / \partial \phi$ is evaluated at $\phi = \phi_0$, and $\mathbf{c} = -\mathbf{C}\phi_0$ is a column vector. Thus, under the above assumptions, the tracking function can be used to provide a linear measurement of, and therefore a means of tracking, the fatigue damage variable ϕ . In [15, 16], a suitably averaged $\mathcal{E}_k(\mathbf{y}(r), \phi)$ was successfully used to track a scalar battery voltage variable.

To actually calculate the PSW tracking function $\mathcal{E}_k(\mathbf{y}(r), \phi)$ for any given initial condition $\mathbf{y}(r)$, we need to know how the fast subsystem evolves over the time interval $k t_s$ for the current value of ϕ , as well as how this subsystem *would have* evolved for the reference value of ϕ_0 . Since the system's fast-time behavior for the current value of ϕ is directly measurable (i.e., we can reconstruct the fast-time trajectory using a sensor measurement from the fast subsystem), then the strategy will be to compare it to the predictions of a *reference model* describing the fast system's behavior for $\phi = \phi_0 + \mathcal{O}(\epsilon)$. Here, the local linear models are used as the simplest form of a globally nonlinear reference model

$$\mathbf{y}(r+1) = \mathbf{A}\mathbf{y}(r) + \mathbf{a}, \quad (5)$$

where \mathbf{A} is an $n \times n$ matrix and \mathbf{a} is an $n \times 1$ vector. Eq. (5) approximates Eq. (2) for a particular point $\mathbf{y}(r)$ in the reference system's reconstructed phase space. Note that in practical applications other modeling solutions, such as neural nets or auto regressive moving averages, may be more appropriate. The parameters of local linear models are determined by calculating the best linear fit between N nearest neighbors of $\mathbf{y}(r)$ and their future states. Then the PSW tracking function (Eq. 3) for the initial point $\mathbf{y}(r)$ can be written as

$$\begin{aligned} \mathcal{E}_k(\mathbf{y}(r), \phi) &= \mathbf{y}(r+k) - \mathbf{A}^k \mathbf{y}(r) - \mathbf{a}^k + \mathbf{E}^M(\mathbf{y}(r)) \\ &= \mathbf{E}_k(\mathbf{y}(r), \phi) + \mathbf{E}^M(\mathbf{y}(r)), \end{aligned} \quad (6)$$

where $\mathbf{E}^M(\mathbf{y}(r))$ represents the local linear model error, and

$$\mathbf{E}_k(\mathbf{y}(r), \phi) = \mathbf{y}(r+k) - \mathbf{A}^k \mathbf{y}(r) - \mathbf{a}^k \quad (7)$$

is the estimated tracking function that can be determined experimentally. The use of $\mathbf{E}_k(\mathbf{y}(r), \phi)$ in place of $\mathcal{E}_k(\mathbf{y}(r), \phi)$ is justified if \mathbf{E}^M is small compared to \mathbf{E}_k .

MULTIDIMENSIONAL DAMAGE DIAGNOSIS

In previous work [15–17], a suitable norm of the averaged value of the estimated tracking function over one data record

$\|\mathbf{E}(\mathbf{y}(r), \phi)\|$ provided a good tracking metric for scalar damage variables. However, as discussed in detail in [15], in general there will be fluctuations in the estimated tracking function caused by two main sources not related to changes in the damage ϕ : (1) changes in the model fit error \mathbf{E}^M from point to point in phase space; and (2) changes in the actual mapping of Eq. (2), also from point to point. In [15], these fluctuations were reduced by an appropriate probability density weighted average.

Multidimensional Damage Tracking Metric

The new approach is to evaluate the average value of the estimated tracking function in N_e disjoint regions \mathcal{B}_i ($i = 1, \dots, N_e$) of the reconstructed phase space to obtain a *multi-dimensional damage tracking metric*:

$$\mathbf{S}_k(\phi) = \bigcup_{i=1}^{N_e} \|\mathcal{B}_i\|^{-1} \sum_{\mathbf{y}(r) \in \mathcal{B}_i} \mathbf{E}(\mathbf{y}(r), \phi), \quad (8)$$

where each data record will have a total of $N_s = d \times N_e$ ($\mathbf{S}_k \in \mathbb{R}^{N_s}$) statistics. In addition to the ability to track multidimensional damage variables, this new metric has an added benefit of compensation for the fluctuation in population of data points. Furthermore, this approach effectively uses all of the data available within one data record, making the damage estimates more robust.

It is conjectured based on Eq. (4) that there is an affine projection $\mathcal{V}_\phi: \mathbb{R}^{N_s} \rightarrow \mathbb{R}^m$ that maps the proposed metric onto the damage state $\phi \in \mathbb{R}^m$:

$$\phi = \mathbf{V}\mathbf{S}_k + \mathbf{v}, \quad (9)$$

where ϕ is an estimate of actual damage state, \mathbf{V} is an $m \times N_s$ matrix, and \mathbf{v} is an $m \times 1$ vector.

Affine projection parameters, \mathbf{V} and \mathbf{v} , can be determined if independent measurements of damage state are available. In an experiment, a total of N_r data records are collected and an $N_s + 1 \times N_r$ matrix \mathbf{W} is formed, such that $\mathbf{W}^i = [(\mathbf{S}_k^i)^T \mathbf{1}]^T$ for each data record $i = 1, \dots, N_r$. Then if an $m \times N_r$ matrix Φ is formed, where $\Phi_i = \langle \phi \rangle_i$ is composed of the average values of ϕ for each data record i , the needed affine transformation can be calculated in the mean squares sense:

$$[\mathbf{V}, \mathbf{v}] = \Phi \mathbf{W}^T (\mathbf{W} \mathbf{W}^T)^{-1}. \quad (10)$$

In many practical situations we do not have the direct measurement of damage state or means to estimate the affine projection parameters of Eq. (10). Therefore, the damage tracking metric has to be used directly to determine the observable facts

about the hidden damage state. Here, we focus on two different approaches to this problem. The first is based on proper orthogonal decomposition [21] of tracking metric statistics, and the second on the optimal damage tracking method [22].

Proper Orthogonal Decomposition Based Damage Identification

Proper Orthogonal Decomposition (POD) or Karhunen-Loève Decomposition has been widely used to estimate the number of active states in nonlinear dynamical systems [21]. Proper orthogonal modes (POMs) have also been instrumental in studying linear and nonlinear mode interactions in systems. Damage evolution, even in linear materials, is a highly nonlinear process. Therefore, POD of the estimated tracking metric should identify the active damage modes (i.e., POM with highest energy content or a mode corresponding to the largest singular values of the tracking metric matrix $[\mathbf{S}_k^i]$).

Thus, we hypothesize that the POD analysis will reveal the number of active damage states in the experiment. In other words, for m active damage modes only m dominant POMs will be identified, and these POMs will be within a linear transformation of actual damage modes.

Optimal Tracking Based Damage Identification

The optimal tracking method [22] relies on the existence of underlying deterministic behavior of the damage accumulation process, but does not require its model. This method is based on maximizing smoothness and overall variation in the observer metric, found by solving a generalized eigenvalue problem. For completeness we give a brief description of the procedure in the following paragraphs.

The tracking metric \mathbf{S}_k , Eq. (8), is estimated for N_r data records. They are arranged in a $N_r \times N_s$ matrix \mathbf{Y} . Each column of this matrix is normalized by subtracting its mean, and scaling it to unit norm. Next, we identify a linear projection of the matrix \mathbf{Y} , $\varphi = \mathbf{Y}\mathbf{c}$ that varies smoothly. This can be accomplished by defining $(N_r - 1) \times N_s$ derivative matrix \mathbf{D} for two-point forward-difference formula, and minimizing the following ratio with respect to \mathbf{c}

$$g(\varphi) := \frac{\|\mathbf{D}\varphi\|^2}{\|\varphi\|^2}. \quad (11)$$

In minimizing g we maximize the smoothness and the overall variation of damage observer φ . The minimum of g is the smallest generalized eigenvalue of

$$[\mathbf{A}, \mathbf{B}] = [(\mathbf{D}\mathbf{Y})^T \mathbf{D}\mathbf{Y}, \mathbf{Y}^T \mathbf{Y}]. \quad (12)$$

The corresponding generalized eigenvector yields the optimal \mathbf{c} and, hence, φ . It should be mentioned that in the original paper [22] this procedure was used to track a scalar variable. However, in this paper this method is extended to track several damage variables. Our hypothesis is that in the presence of m -dimensional damage evolution we would yield m generalized eigenvalues of Eq. (12) that will be several magnitudes of order smaller than the rest; the corresponding φ will be within a linear transformation of the actual damage state variable ϕ .

MODEL OF AN ELECTROMECHANICAL SYSTEM

In [15, 16] we described an experimental apparatus, which was a constrained version [23] of a vibrating beam in the force field of two permanent magnets. The only difference with the previous system was that one permanent magnet was augmented by an electromagnet. In this paper, *both* permanent magnets are outfitted with identical electromagnets. The force field at the beam tip drifts as the batteries powering the electromagnets discharge. The model parameters are chosen so that a complete discharge of the batteries manifests itself in about a 3.5% change in the natural frequencies of small oscillations in each electromagnet's well.

As in [16] the experimental system can be viewed as a mechanical subsystem coupled with an electromagnetic subsystem. The derivation of the mathematical model is identical to one presented in [16], with the exception of one additional electromagnet circuit. Therefore, without going into details, we present a final dimensionless form of the equations of motion for the beam vibration

$$\ddot{\theta} + \mu \dot{\theta} + (1 - \alpha_1) \theta + \alpha_3 \theta^3 + \sum_{i=1}^2 \frac{\kappa L_r (\theta - \lambda_i)}{(1 + \kappa (\theta - \lambda_i)^2)^2} \psi_i^2 = f \cos \Omega t. \quad (13)$$

This equation is coupled to a set of equations (for $i = 1, 2$) describing the current flow in the electromagnets' circuits:

$$\left[1 + \frac{L_r}{1 + \kappa (\theta - \lambda_i)^2} \right] \dot{\psi}_i + \left[r - \frac{2 \kappa L_r (\theta - \lambda_i) \dot{\theta}}{[1 + \kappa (\theta - \lambda_i)^2]^2} \right] \psi_i = \phi_i. \quad (14)$$

In Eqs. (13–14) θ , ψ_1 and ψ_2 represent fast-time dynamic variables describing beam displacement and electrical oscillations; μ accounts for mechanical viscous damping; α_1 and α_3 describe the shape of the potential field; κ indicates the strength of the coupling between the mechanical and electrical oscillations; L_r describes the electromagnets' inductance; $\lambda_1 = -\lambda_2$ indicate the position of the electromagnets; f is a forcing amplitude; Ω

is a ratio of forcing and natural frequencies; r describes the total resistance of the circuits; and ϕ_1 and ϕ_2 represent slow-time damage variables or the dimensionless battery voltages.

The time evolution of the battery voltage is governed by electrochemical processes, which are not explicitly modeled. Instead, given the experimental battery voltage evolution trends typically seen in the experiments [15], the following voltage evolution law for both batteries is used,

$$\dot{\phi}_i = -\epsilon_i (\phi_i - \xi) \left(1 + \gamma (\phi_i - \eta)^2\right) \quad (i = 1, 2), \quad (15)$$

where ξ , γ and η are positive constants, and the rate constant ϵ_i satisfies $0 < \epsilon_i \ll 1$.

From the experimental results [15] we know that the internal battery voltage initially drops rapidly to the operating range and remains there for an extended period, slowly decreasing before another rapid drop to near zero voltage at the end of the battery's life. The form of Eq. (15) is the simplest rate law, which exhibits these characteristics.

Equations (13–15) were integrated numerically with a standard fourth-order variable-step-size Runge-Kutta algorithm. Since this study was inspired by the experimental investigation of a scalar damage tracking method, the parameters for the model were selected to match the properties of the experimental system in key ways, as described below.

It is assumed that fully charged batteries provide 9 V DC power. It is also assumed that the natural frequency of small oscillations in the potential well with the electromagnet changes by 3.5 percent from 8.8 Hz to 8.5 Hz. The effective mass, $m = 0.2$ kg, and length, $l = 0.128$ m, were obtained directly from the experiment. A fourth-order polynomial fit to a histogram of the experimental reference data was used to estimate $\alpha_1 = 2.6558$ and $\alpha_3 = 0.8805$. The effective damping parameter was assumed to be $\mu = 0.088$.

By linearizing Eqs. (13), and (14) about the stable equilibria ($\theta = \pm\sqrt{(\alpha_1 - 1)/\alpha_3}$) for $\Phi = 0$, expressions for the frequency of small oscillations were obtained, which were used to estimate the effective stiffness k . Since the frequency for $\Phi = 0$ in both electromagnets' wells is 8.5 Hz, one can estimate $k = 0.071$ using m , l , and α_1 . We chose $\kappa = 0.746$, so that the effect of L_r on inductance amplitude decreased to 10 percent at 2λ distance. To determine other parameters, the case of $\Phi_1 = 9$ and $\Phi_2 = 0$ was considered, for which the natural frequency in the powered electromagnet's well is 8.8 Hz. Using this information, we found $L_r = 0.079$ after arbitrarily setting $r = 10$. Forcing amplitude $f = 1$ and forcing frequency $\Omega = 1.95$ were chosen so that the system exhibited nominally chaotic motion throughout the experiment.¹

¹No tests for chaos were performed for these numerical experiments, since the existence or nonexistence of chaos is not particularly relevant to the task at hand.

Other parameters used in the simulations were $\eta = 22$, $\gamma = 1$ and $\xi = 0.1$. The rate parameters for battery evolution laws were chosen to be $\epsilon_1 = 1 \times 10^{-6}$ and $\epsilon_2 = 0.5 \times 10^{-6}$, so that the first battery discharged twice as fast as the second. Using the above parameters, one has $\phi = 2.846 \Phi$, and the observed fast-time dynamics of the simulated θ were found to have qualitatively similar trajectories in the $(\theta, \dot{\theta})$ phase space to those observed with experimental strain-gauge time series.

RESULTS OF DAMAGE IDENTIFICATION

The total of 3×10^6 data points for each state variable were collected with a sampling time of $t_s = 0.1$ during the numerical integration of Eqs. (13–15). At the end of the simulation, both ϕ_1 and ϕ_2 variables reached a ξ value. For damage identification purposes, only the beam angular displacement θ time series was used. After waiting an initial period to allow transients to die off, the first 2^{14} data points of the scalar θ data set were used for the reference model. Average mutual information and false nearest neighbors algorithms were used to select a delay of $\tau = 7$ sample steps, and an embedding dimension of $d = 6$ for the reference data set. The average pointwise dimension of the reference data set was approximately 2.7, supporting our assumption of a nominally chaotic system.

For the tracking metric S_1 , Eq. (9), the entire reconstructed data set was divided into consecutive data records of size 2^{12} points each (i.e., $M = 2^{12}$ and $N_r = 732$), and the sixteen nearest neighbors were used for the reference model construction. The reconstructed reference phase space was partitioned into sixteen disjoint regions uniformly distributed along the third coordinate of the reconstructed state vectors. The middle coordinate was used to circumvent any edge effects present in the reconstruction. The tracking metric was determined by evaluating the tracking function in each of these partitions. Thus, the 96×732 tracking metric matrix \mathbf{Y} was formed. The metric matrix \mathbf{Y} was normalized by subtracting the mean from each row and scaling it to the unit norm. Some dominant trends were observed in these components. However, some large local fluctuations in all the components of the metric were also present. These are the result of changes in the initial point population from one data record to another. By itself, this change is the result of our system going through bifurcations as hidden slow parameters drift.

The affine transformation of Eq. (9) was determined using Eq. (10). Results of this calculation are plotted in Fig. 1. The graphs in the right column of this figure show the estimated (thin gray line) and actual (dashed black line) battery voltages versus time; in the left column the calibration curves are shown, where estimated battery voltages are plotted versus corresponding true battery voltages. The dashed straight line in the calibration figures shows the corresponding linear fit to the data. The accuracy of these estimates can be further improved by accounting for the precision of the local linear model when calculating S , Eq. (8),

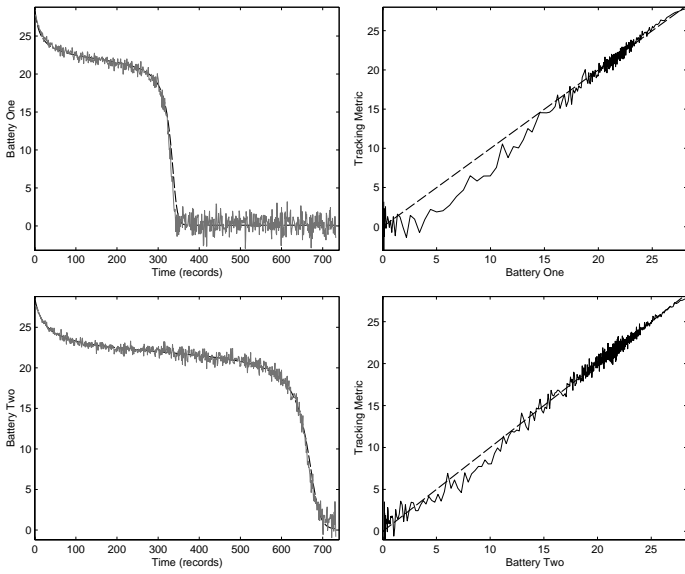


Figure 1. [left column] Affine projection of the damage tracking metric (gray lines) and actual battery voltage (dashed lines) versus time. [right column] Corresponding calibration curves (black lines) with least-squares linear fit (dashed lines).

as shown in [15]. However, this is left for future development.

In many practical situations, the direct measurement of a damage state is not available, and one is forced to infer the facts about this hidden damage state from the available statistics. Therefore, for damage identification purposes, the tracking data was analyzed using POD and optimal tracking methods. In this analysis we do not expect to find the exact curves shown in Fig. 1. These curves are just one particular projection of the two-dimensional damage accumulation curve. However, as hypothesized, we expect to find other equivalent projections of this curve that are linear transformations of the original.

The results of POD calculations are shown in Fig. 2 (a), (b), and (c). Fig. 2(a) shows the first fifteen singular values of matrix \mathbf{Y} . In this figure, first two singular values are clearly separated from the rest; however, they are not significantly larger than the rest. In Fig. 2 (b) and (c) the corresponding first two POMs are shown. The amount of local fluctuation in these modes is considerably smaller compared to the graphs in Fig. ???. However, the existence of a large periodic window in data records 625–635 produces a noticeable kink in the trend that is not attributed to the damage evolution.

The results of the application of the optimal tracking method to the tracking matrix \mathbf{Y} are shown in Fig. 2 (d), (e), and (f). The first fifteen generalized eigenvalues of $[\mathbf{A}, \mathbf{B}]$, Eq. (12), are depicted in Fig. 2 (d). Here, the first two generalized eigenvalues are clearly several orders of magnitude smaller than the rest. The optimal tracking modes (OTMs) that correspond to these first

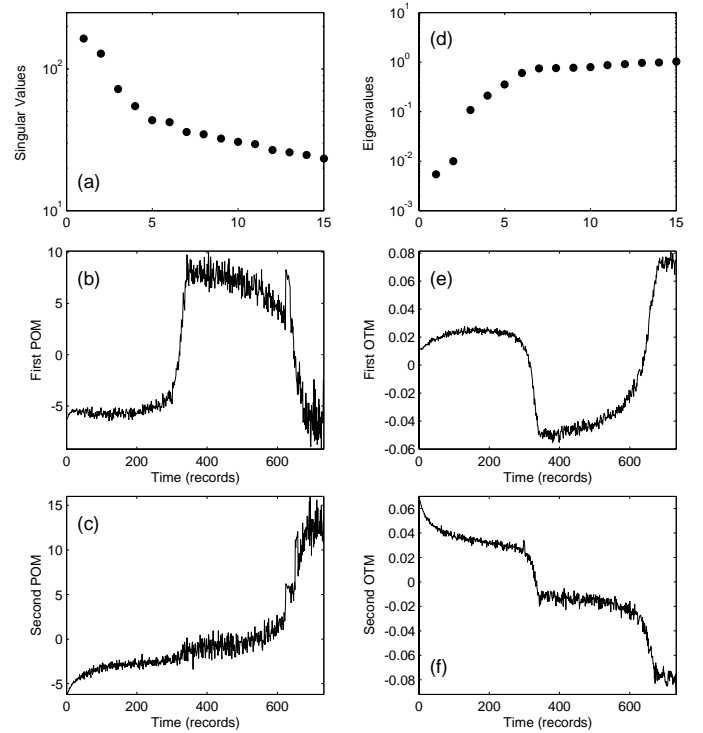


Figure 2. (a) First fifteen singular values of damage tracking metric \mathbf{Y} . (b) and (c) Proper orthogonal modes corresponding to the first two singular values. (d) First fifteen generalized eigenvalues of $[\mathbf{A}, \mathbf{B}]$, Eq. (12). (e) and (f) Optimal tracking modes corresponding to the first two generalized eigenvalues.

two eigenvalues are shown in Fig. 2 (e) and (f), respectively. In these modes, the local fluctuations are greatly reduced compared to both the POMs shown in Fig. 2(a–c) and the tracking metric components in Fig. ???. In addition, these graphs do not suffer from the presence of large periodic windows in the data records and provide consistent trends that can be directly related to the damage evolution curves.

Both the POD and optimal tracking methods yield virtually identical trends. However, the underlying trend is more pronounced in the optimal tracking calculation, which has significantly lower local fluctuations and does not suffer from changes unrelated to damage evolution. Therefore, in further analysis only these two OTMs are used.

The affine transformation relating the first two OTMs to the actual damage variables was determined in the least-squares sense. The result of this calculation is shown in Fig. 3. The graphs in the right column of this figure show POMs after the affine transformation and actual battery voltage plotted versus time; the left column shows the corresponding calibration curves, where the OTM based tracking observers are plotted versus actual battery voltages. The straight dashed line in these figures

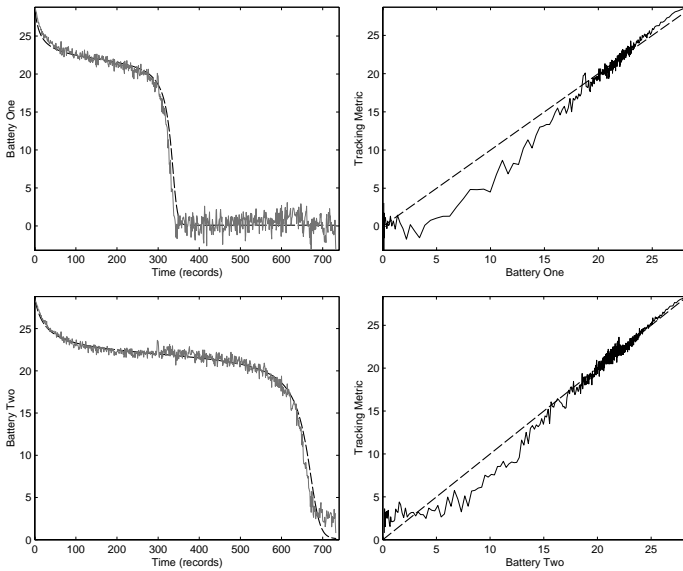


Figure 3. [left column] Scaled OTMs (gray lines) and actual battery voltage (dashed lines) versus time. [right column] Corresponding calibration curves (black lines) with least-squares linear fit (dashed lines).

shows the corresponding linear fit to the data.

DISCUSSION

The tracking results based on the simulated experiment show that the tracking algorithm accurately recovers (within an affine projection) the theoretical tracking curves for both simultaneously evolving damage variables, as shown in Fig. 1. This confirms our conjecture that the tracking metric \mathbf{S} can be projected onto the damage state variable ϕ using Eq. (9). The local fluctuations present in this tracking metric are the result of changes in the population of points from data record to data record and the inaccuracy of the local linear models. These results can be further improved by incorporating probability density function weighted averages as in [15], and using stochastic interrogation [23] to maximize uniformity of point populations within separate data records.

Another hypothesis was that the POD and optimal tracking analysis would yield a proper number of active damage modes. The results conclusively confirmed that this is indeed true for the identified OTMs and, to a lesser extent, for the identified POMs. The generalized eigenvalues calculated in the optimal tracking procedure clearly identified the two most dominant modes that satisfied *optimality criteria*, which were maximization of smoothness and overall variation. However, the singular values obtained in POD analysis were not as clearly differentiating. It was apparent that a significant amount of energy was still present in the higher POMs.

Our final hypothesis was that the identified POMs and OTMs are within an affine transformation of the actual damage states. Both the first two POMs and OTMs showed strikingly similar trends. However, the OTMs had significantly smaller local fluctuations and did not suffer from the drastic change in fast-time system dynamics. Their linear transform provided an accurate tracking observer for the actual damage variables as shown in Fig. 3. In fact, these graphs are virtually identical to the graphs obtained using the affine projection of \mathbf{S} in Fig. 1. The differences are only noticeable for very large changes in the damage variables. Therefore, identified OTMs provide accurate and consistent multidimensional damage observers.

CONCLUSIONS

In this paper, a novel multi-mode damage diagnosis method was presented. The multidimensional damage tracking metric was developed in the framework of a dynamical systems approach to damage evolution. This methodology does not depend on knowledge of particular damage physics. Instead, it provides experimental means to determine practically observable and observed facts of damage accumulation. The procedure implicitly uses the assumption that the system undergoing damage accumulation possesses time-scale separation, where damage accumulation occurs on a much slower time scale than the observable dynamics of a system.

A detailed description of the damage tracking algorithm was given. Experimental procedures for estimating tracking functions in a reconstructed phase space, calculation of the multi-dimensional tracking metric, and appropriate damage observers were given before describing an application to a simulated experimental system. A mathematical model of a harmonically driven cantilever beam in a force field of two battery-powered electromagnets was used in the simulation. Terminal voltages of the discharging batteries were treated as the slow-time damage variables, and the angular displacement of the vibrating beam was considered to be the measurement of the fast-time dynamics. An empirical battery discharge model was used to describe the slow-time damage evolution.

The beam angular displacement data was used to reconstruct the phase space of the fast-time dynamics using a delay coordinate embedding. Initial fast-time data was used to build a database reference model predicting short-time evolution of trajectories in the reconstructed phase space. The PSW tracking metrics were evaluated in this reconstructed phase space by comparing the current fast-time trajectories to the predictions of the reference model. As the damage grew, the system underwent many bifurcations causing repeated periodic/chaotic transitions. Nevertheless, the affine projection of the calculated damage tracking metric was shown to accurately track the two-dimensional damage states corresponding to simultaneously discharging battery voltages.

The practical applicability of the method was validated by two different methods of damage identification. Both the optimal tracking and proper orthogonal decomposition methods provided similar trends. However, the optimal tracking method was less susceptible to the effects of change in the directly observable dynamics and had a significantly better signal-to-noise ratio. It showed that only two optimal tracking modes satisfied the optimality criterion. These identified modes were shown to be within a linear transform from the actual two-dimensional damage variable and provided accurate damage observers.

ACKNOWLEDGMENT

This work was supported by the NSF CEREER grant No. CMS-0237792 and University of Rhode Island Council for Research Grant.

REFERENCES

- [1] Zou, Y., Tong, L., and P., S. G., 2000, "Vibration-based model-dependent damage (delimitation) identification and health monitoring for composite structures – a review," *J. Sound & Vib.*, **230** (2), pp. 357–378.
- [2] Worden, K., Manson, G., and Fieller, N. R. J., 2000, "Damage detection using outlier analysis," *J. Sound & Vib.*, **229** (3), pp. 647–667.
- [3] Luo, G. Y., Osypiw, D., and Irle, M., 2000, "Real-time condition monitoring by significant and natural frequencies analysis of vibration signal with wavelet filter and autocorrelation enhancement," *J. Sound & Vib.*, **236** (3), pp. 413–430.
- [4] Craig, C., Neilson, D., and Penman, J., 2000, "The use of correlation dimension in condition monitoring of systems with clearance," *J. Sound & Vib.*, **231** (1), pp. 1–17.
- [5] K., M. C., 1998, "Objective machinery fault diagnosis using fuzzy logic," *J. Sys. and Sig. Proc.*, **12** (6), pp. 855–862.
- [6] Swanson, D. C., Spencer, J. M., and Arzoumanian, S. H., 2000, "Prognostic modelling of crack growth in a tensioned steel band," *Mech. Sys. & Sig. Proc.*, **14** (5), pp. 789–803.
- [7] Natke, H. G., and Campel, C., 1997, *Model-Aided Diagnosis of Mechanical Systems: Fundamentals, Detection, Localization, Assessment*, Springer-Verlag, Berlin.
- [8] Loparo, K. A., Adams, M. L., and Lin, W., 2000, "Fault detection and diagnosis of rotating machinery," *IEEE trans. Indust. Elect.*, **47** (5), pp. 1005–1014.
- [9] Dron, J., Rasolofondraibe, L., Couet, C., and Pavan, A., 1998, "Fault detection and monitoring of a ball bearing benchtest and a production machine via autoregressive spectrum analysis," *J. Sound & Vib.*, **218** (3), pp. 501–525.
- [10] Wang, W., and Wong, A. K., 2002, "Autoregressive model-based gear fault diagnosis," *J. Vib. & Acoustics*, **124** (2), pp. 172–179.
- [11] Sampaio, R. P. C., Maia, N. M. M., and M., S. J. M., 1999, "Damage detection using the frequency-response-function curvature method," *J. Sound & Vib.*, **226** (5), pp. 1029–1024.
- [12] Worden, K., 1997, "Structural fault detection using a novelty measure," *J. Sound & Vib.*, **201** (1), pp. 85–101.
- [13] Cornwell, P., Doebling, S., and Farrar, C., 2000, "Application of the strain energy damage detection method to plate-like structures," *J. Sound & Vib.*, **224** (2), pp. 359–374.
- [14] Cusumano, J. P., and Chatterjee, A., 2000, "Steps towards a qualitative dynamics of damage evolution," *Int. J. Solids & Struct.*, **37** (44), pp. 6397–6417.
- [15] Chelidze, D., Cusumano, J. P., and Chatterjee, A., 2002, "Dynamical systems approach to damage evolution tracking, part 1: Description and experimental application," *J. Vib. & Acoustics*, **124** (2), pp. 250–257.
- [16] Cusumano, J. P., Chelidze, D., and Chatterjee, A., 2002, "Dynamical systems approach to damage evolution tracking, part 2: Model-based validation and physical interpretation," *J. Vib. & Acoustics*, **124** (2), pp. 258–264.
- [17] Chelidze, D., and Cusumano, J. P., 2003, "A dynamical systems approach to failure prognosis," *accepted, J. Vib. & Acoustics*.
- [18] Sauer, T., Yorke, J. A., and Casdagli, M., 1991, "Embedology," *J. Stat. Phys.*, **65** (3-4), pp. 579–616.
- [19] Fraser, A. M., and Swinney, H. L., 1986, "Independent coordinates for strange attractors from mutual information," *Phys. Rev. A*, **33** (2), pp. 1134–1140.
- [20] Kennel, M. B., Brown, R., and Abarbanel, H. D. I., 1992, "Determining embedding dimension for phase-space reconstruction using a geometric construction," *Phys. Rev. A*, **45** (6), pp. 3403–3411.
- [21] Berkooz, G., Holmes, P., and Lumley, J. L., 1993, "The proper orthogonal decomposition in the analysis of turbulent flows," *Annual Review of Fluid Mechanics*, **25**, pp. 539–575.
- [22] Chatterjee, A., Cusumano, J. P., and Chelidze, D., 2002, "Optimal tracking of parameter drift in a chaotic system: Experiment and theory," *J. Sound & Vib.*, **250** (5), pp. 877–901.
- [23] Cusumano, J. P., and Kimble, B., 1995, "A stochastic interrogation method for experimental measurements of global dynamics and basin evolution: Application to a two-well oscillator," *Nonlinear Dynamics*, **8**, pp. 213–235.